EMAE 355 Group 7 Project 3 Report: Geothermal Power Plant with CO2 Sequestration

Will MacCormack Owen Braun Julian Town Natalia Parla Rodríguez

May 4, 2024

1 Executive summary

The proposed geothermal power plant with sequestration produces a net power output of 35 kW. The proposed system is comprised of a single injection pipe feeding into the porous formation, in which 3.24kg/s of CO_2 is sequestered. Remaining flow passes through the porous medium, where it is then forced back up to the surface through two outlet pipes. Flow exits each of the two pipes and is filtered to remove contaminants. The near pipe feeds an 0.753 diameter axial turbine spinning at 5400 RPM. The far pipe feeds an 0.679 diameter axial turbine spinning at 5400 RPM. The turbine shafts are connected to gearboxes that reduce the speed to that used in power generation, 3600 RPM. Both turbines need a 3:2 gearbox ratio. The outlet for each turbine is combined in a tee and fed through a heat exchanger with a UA value of 5103 W/K to return the flow to supply conditions. The heat exchanger rejects heat into river water. The outlet flow of the heat exchanger is combined with supply CO_2 and pumped down the injection pipe by a 0.257 m diameter rotary piston pump spinning at 3388 RPM.

2 Problem statement

The main goal of this project is to design a geothermal power cycle to extract energy from the elevated temperature of the underground.

This system must include different components such as turbines, pumps, and heat exchangers, as well as a filtration system to clean the return flow. Each of these elements will be analyzed in the design and will be specified/sized appropriately. The condenser will be specified in terms of UA. The turbines and pump will be defined in terms of rotational speed, impeller diameter, and configuration (axial, radial, etc).

Ultimately, system performance will be evaluated, and the potential of converting CO2 injection wells into geothermal power cycles will be demonstrated, showing a promising solution to simultaneously combat greenhouse gas emissions and generate power.

3 Background

Geothermal power plants exploit the Earth's natural heat to generate electricity, offering a renewable and sustainable energy source. These plants tap into the heat stored beneath the Earth's surface, typically in the form of hot water or steam found in geothermal reservoirs. The heat is extracted through production wells drilled into the reservoirs, and the resulting steam is used to drive turbines, which, in turn, generate electricity. Geothermal power plants come in various configurations depending on the temperature and state of the resource being utilized.

On the other hand, carbon sequestration is a process aimed at capturing carbon dioxide (CO_2) emissions from industrial sources, such as power plants and factories, and storing them underground to prevent release into the atmosphere. The primary goal of carbon sequestration is to mitigate climate change by halting or reversing the increase in the concentration of CO_2 in the atmosphere, thereby reducing the greenhouse effect and its associated impacts.

The depth at which CO_2 is stored underground, along with the surrounding temperature, plays a significant role in the efficacy and power feasibility of carbon sequestration projects. As CO_2 is injected into geological formations, such as deep saline aquifers or depleted oil and gas reservoirs, it encounters which affect its density, viscosity, and solubility in groundwater. At greater depths, temperatures are typically higher, which can enhance the efficiency of CO_2 storage by increasing its

solubility and reducing its viscosity. However, deeper wells require more infrastructure and advanced boring operations to bring the CO_2 to the required depth. Additionally, deeper formations may provide more secure and stable storage conditions over the long term. Moreover, deep sequestration formations that provide high heat sources enable energy extraction from a combined sequestration and power cycle system.

4 Design

The design chosen includes an supply of CO_2 that goes directly to a rotary piston pump with a diameter of 0.257m spinning at 3388 RPM, where it is then pumped down through a copper pipe sleeved in carbon steel and cement until it reaches the underground reservoir. The internal copper pipes facilitate maximum heat transfer into the CO_2 from the soil, while maintaining durability and resistance to corrosion.

After passing through the underground reservoir, the CO_2 exits though two carbon steel pipes sleeved in carbon steel and cement that have two 4900 Series High Flow High Pressure T-Type Norman Filters at the top. These filters are placed in the system to ensure that the CO_2 leaving the formation is clean and free of impurities before it enters the turbines. The filters ensure prevent damage in the turbines, heat exchanger, and pump. Each of the two turbines extracts heat from the CO_2 in one upward pipe. The closer of the turbines to the injectection well is 0.753m in diameter spinning at 5400 RPM. The farther turbine is 0.679m in diameter, also spinning at 5400 RPM. Both turbines will use a gearbox with a 3:2 ratio to reduce the speed to the speed of grid generation at 3600 RPM.

After the turbines, the two CO_2 streams are combined and enter the heat exchanger. The heat exchanger requires a UA value of 5103 W/K to ensure it returns the circulating fluid back to supply conditions by rejecting heat into river water. This CO_2 can then be recycled back into the system for injection, completing the loop.

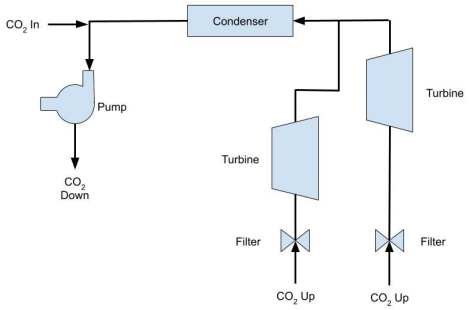

Figure 1: Overall Process Diagram

Overall, this carbon sequestration system, powered by a geothermal heat cycle offers a sustainable and environmentally responsible solution for energy generation while addressing the challenges of climate change and carbon emissions. The overall design can be seen below in Figure 8.

5 Analysis

5.1 Vertical Pipe Analysis

The greatest complexity in analysis of this system is the behavior of the working fluid in the injection and outlet pipes. To determine the properties of the CO_2 along the pipe, it was broken into small sections and each section was sequentially analyzed. For each section the input Temperature, Pressure, and Enthalpy are known, and the output values can be calculated.

5.1.1 Pipe Pressure Analysis

For a given section of Pipe flow, the friction along the pipe causes a pressure drop. The energy from the pressure loss cannot escape the fluid, thus it is converted into thermal energy, which is included in the Thermal Analysis section later. The friction factor is determined from the Colebrook-White equation. Additionally, the pressure increases as a function of depth change.

For a given change in height, δh, the change in pressure in the intake pipe due to depth is

$$\delta P = \rho g \delta h \tag{1}$$

Where ρ is the fluid density and g is gravitational acceleration. δh is negative in the intake pipe, and positive in the two outtake pipes.

Friction in these pipes is not negligible, and the pressure loss due to friction is given below.

$$\delta P = -f \frac{\rho u^2}{2d} |\delta h| \tag{2}$$

Where f is the Darcy Friction Factor, u is the fluid velocity, and d is the pipe diameter. In total, the total pressure change in the intake pipe is

$$\delta P = \rho g \delta h - f \frac{\rho u^2}{2d} |\delta h| \tag{3}$$

For laminar flow, the friction factor is estimated by

$$f = \frac{64}{Re} \tag{4}$$

For turbulent flow, the Darcy friction factor was supplied by the Colebrook-White Equation and implicitly sovled for by Scipy Optimize's root_scalar function. From [1], it was estimated that a reasonable pipe absolute surface roughness of 0.229mm. This value is for a worn pipe as this plant is meant to last for years. This is a reasonable estimate for that situation. Initially, the pressure loss will be less, which boots the projected power production numbers.

$$|\frac{1}{\sqrt{f}}| + 2log_{10}\left(\frac{2.5}{Re * \sqrt{f}} + \frac{\epsilon}{3.71d}\right) = 0 \tag{5}$$

Where ϵ is the absolute surface roughness.

For a small length of pipe, the change can be approximated by Euler's method. The pressure loss in a pipe segment is

$$\Delta P = \rho g \Delta h - f \frac{\rho u^2}{2d} |\Delta h| \tag{6}$$

5.1.2 Pipe Heat Transfer

A prior study of geothermal power found that at 2m, the soil temperature became constant. Therefore, we apply the soil temperature boundary condition to the outside of a 2m thick cylindrical tube of soil.

For a radial geometry, the overall conduction, $\dot{Q}_{cond}$ is given in terms of the thermal conductivity, k, the internal and external radii, r_i and r_o respectively, and the length of the segment, δL by the expression below.

$$\delta\dot{Q}_{cond} = \frac{2\pi k}{ln(\frac{r_o}{r_i})}\Delta T\delta L \tag{7}$$

Thus, the radial thermal resistance for a cylinder for a given pipe length is

$$R_{cond} = \frac{ln(\frac{r_o}{r_i})}{2\pi k\delta L} \tag{8}$$

For each material of the pipe wall, the thermal conductivity, internal radius, and external radius differ. The values for each are summarized below in Table 1

Section	**Thermal Conductivity (W/m^2K)**	**Internal Radius (m)**	**External Radius (m)**
Soil	1	0.707	2
Inner Tube (Down)	401	0.0254	0.0302
Inner Tube (Up)	45	0.0254	0.0302
Concrete	2.25	0.0302	0.127
Outer Casing	45	0.127	0.0707

Table 1: Pipe Thermal and Geometric Parameters

The soil thermal conductivity was first estimated by determining the type of soil present in Los Angeles, which was determined to be mostly sandy from [3]. From this knowledge, the thermal conductivity was estimated to be approximately 1, depending on the water content of the soil [4]. The external radius for soil conduction was taken from a study done by Guan et. al. [2], who analyzed the heat diffusion of a home geothermal pipe system. The pipe analyzed was also vertical. It was determined that the pipe affected the soil up to a distance of approximately 1 meter. A factor of safety of two was included to account for the fact that the soils and temperatures of the two locations were different. This results in a more conservative estimate, which is allowable because having the temperature converge to the constant value within this radius does not affect any system parameters. Beyond this distance of 2m, the soil is considered to be constant surface temperature regardless.

The soil temperature as a function of depth was provided, where h is measured in kilometers, and the temperature is in Celsius.

$$T = 62.5|h| + 20 \tag{9}$$

The general expression for convection is given below, and depends on the diameter, temperature difference, length, and convection coefficient, h.

$$\delta\dot{Q}_{conv} = hA\Delta T = h(2\pi r\delta L)\Delta T \tag{10}$$

The thermal resistance for conduction then is

$$R_{conv} = \frac{1}{2\pi r h \delta L} \tag{11}$$

The internal flow coefficient, h, is related to the Nusselt Number, a dimensionless parameter that relates the relative strength of fluid convection to conduction. It is given by:

$$h = \frac{Nuk_f}{d} \tag{12}$$

The internal flow convection for the pipes are based on the assumption of constant surface temperature for a segment, since the length is sufficiently small. The relation for internal Convection depends on flow regime. The critical value is Re = 2,300. For laminar flow, the relation is

$$Nu = 3.66 \tag{13}$$

For turbulent flow, the relation for fluid heating is

$$Nu = 0.023 Re^{4/5} Pr^{0.4} \tag{14}$$

And then for fluid cooling,

$$Nu = 0.023 Re^{4/5} Pr^{0.3} \tag{15}$$

These parameters are used to find the total thermal resistance, R_{tot}.

$$R_{tot} = R_{conv} + \sum_{i=1}^{3} R_{cond,i} \tag{16}$$

This was used to find the the heat flux given the fluid and soil temp for a segment.

$$\dot{Q} = \frac{T_s - T_f}{R_{tot}} \tag{17}$$

The heat transfer due to frictional loss is given by the equation below. it is assumed that all frictional losses are converted to thermal energy.

$$\delta \dot{Q}_{fric} = \dot{m} f \frac{u^2}{2d} \delta L \tag{18}$$

Therefore, the total increase in internal energy of the fluid is given by the expression

$$\delta U = \frac{\delta \dot{Q}_{cond}}{\dot{m}} + \frac{\delta \dot{Q}_{fric}}{\dot{m}} \tag{19}$$

Like in the expression for pressure loss, with a small enough step size the segmented approximation will approach the continuous solution.

$$\Delta U = \frac{\Delta \dot{Q}_{cond}}{\dot{m}} + \frac{\Delta \dot{Q}_{fric}}{\dot{m}} \tag{20}$$

The provided starting fluid temperature and pressure are summarized in Table 2 below. Coolprop was used to determine the fluid state.

Temperature (°C)	**Pressure (MPa)**	**Fluid State**
20	6	Liquid

Table 2: CO_2 Initial Properties

This results in fluid properties entering the porous reservoir are summarized in Table 6 below.

Fluid Property	Input
Pressure (MPa)	26.4
Temperature (C)	66.8
Specific Heat Capacity (J/KgK)	2148

Table 3: Porous Formation Input and Output Parameters

5.2 Porous Formation

The behavior of the fluid in the porous formation was provided.

5.2.1 Pressure Loss

The pressure drop across the formation is governed by the following expression,

$$\dot{V} = \frac{\kappa A(P_{in} - P_{out})}{\mu L} \tag{21}$$

Where V' is the volumetric flow rate, κ is the permeability of the porous medium, μ is the dynamic viscosity, and L is the length between the two pipes. All fluid in the pipe enters the porous medium, and the provided area was $2m^2$. Rearranging, the pressure at the entrance of an outtake pipe is,

$$P_{out} = P_{in} - \frac{\dot{m}\mu L}{\rho\kappa A} \tag{22}$$

The parameters used in the calculation are summarized below in Table 4

Outlet 1 Distance (m)	Outlet 2 Distance (m)	Permeability (m^2)	Area (m^2)
70	112	10^{-11}	2

Table 4: CO_2 Initial Properties

5.2.2 Heat Transfer

Heat transfer through the porous medium was also considered. The equation provided is given below, Where T_s is the temperature at depth, T_i is the temperature of the flow entering the reservoir, T_o is the temperature exiting the flow, P is the equivalent perimeter, and Cp is the average specific heat at a constant pressure. The Cp at the entrance and exit were evaluated at the given properties.

$$\frac{T_s - T_o}{T_s - T_i} = e^{\frac{-PhL}{m'Cp}} \tag{23}$$

Rearranging, the exit temperature of a pipe is given by the expression

$$T_o = T_s - (T_s - T_i)e^{\frac{-PhL}{m'Cp}} \tag{24}$$

The perimeter in this case is the equivalent perimeter of a circular pipe with the same area as the porous formation. The $2m^2$ area is assumed to be a circular pipe for the calculation. The effective heat transfer coefficient, h, was once again calculated using the Nusselt Number. The Nusselt number was provided, at a value of 450.

The porous medium absorbs part of the mass flow rate through sequestration. This value was provided to be $3.24 kg/s$.

The constant parameters in the heat transfer analysis are summarized in Table 5 below.

Outtake 1 Distance (m)	Outtake 2 Distance (m)	Perimeter (m)
70	112	5.013

Table 5: CO_2 Initial Properties

This results and fluid properties entering the porous reservoir are summarized in the table below.

State	Input	Outtake at 70m	Outtake at 112m
Pressure (MPa)	26.5	21.3	19.9
Temperature (C)	66.8	220	220

Table 6: Porous Formation Input and Output Parameters

5.3 Filter Analysis

In order to remove any contaminants or obstructions in the flow two filters were placed in front of the turbines. Two Norman Filter 4900 Series High Flow High Pressure T-Type filters were chosen [6]. These filters are rated for 150 GPM, 8000 psi and 300 °F which are well above our operating conditions of approximately 135 GPM and 1500 psi. Additionally, a glass fiber filter with elements sized at 1 micron was selected. This will protect the turbines from a variety of particles encountered including silk and sand. The pressure drop across the filter was deemed negligible by examining [6]. Looking at 2 for a highly viscous substance such as oil a maximum pressure drop of about 45 psi is expected around a flow rate of 135 GPM. Thus, the pressure drop across the filter for a significantly less viscous fluid, like CO_2 will be much less and can be considered negligible compared to the static pressure of 1500 psi before the filter/turbine.

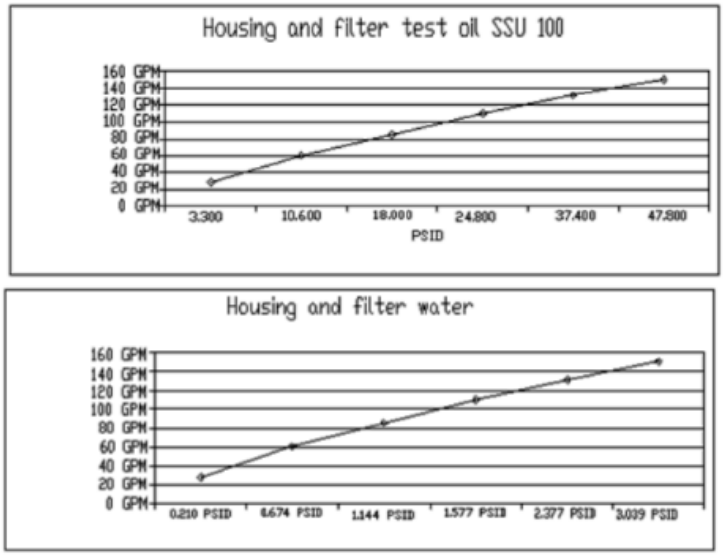

Figure 2: 4900 Series Pressure Drop

5.4 Above Ground Piping

Above ground piping was assumed to be isobaric and adiabatic as piping layout was out of scope of this project.

5.5 Turbine and Pump Analysis

The work for the turbine and pump were both calculated by enthalpy. A pump was selected because the supply conditions result in liquid CO_2. Given the entrance enthalpy, h_{in}, the exit enthalpy, H_{out} , and the mass flow rate, the net work is given by the following expression

$$\dot{W} = \dot{m}(h_{out} - h_{in}) \tag{25}$$

The isentropic efficiency of the pump and the turbine were assumed to be 0.85.

5.5.1 Pump Fluid Condition

Secondly, the compressor input pressure (and thus the turbine output pressures) were fixed to the input pressure from the outtake pipes. The pump output pressure was varied to maximize the output power. The mass flow rate of the pump is greater than the mass flow rate of the turbine by the mass flow lost to sequestration.

The enthalpy after the pump is a function of isentropic efficiency, η_p and different enthalpy states.

$$\eta_p = \frac{h_{2s} - h_1}{h_2 - h_1} \tag{26}$$

Where h_{2s} is the enthalpy at state 2 given constant entopy. The Pressure at state 2 is the other known variable, though it changes through the optimization process. The input pressure and temperature of the pump are fixed by the final values from the outtake pipes, giving h_1. The input pressure of the turbine is the output pressure of the pump at the temperature exiting the heat exchanger. Solving for h_2,

$$h_2 = h_1 + \frac{h_{2s} - h_1}{\eta_p} \tag{27}$$

Likewise, for the turbine, the isentropic efficiency is given by the expression

$$\eta_t = \frac{h_1 - h_2}{h_1 - h_{2s}} \tag{28}$$

Solving for the actual enthalpy in the second state,

$$h_2 = h_1 - \eta_t(h_1 - h_{2s}) \tag{29}$$

The heat transfer for the heat exchanger is also necessary to determine. It is assumed that the work done in these devices is negligible.

5.5.2 Heat Exchanger Analysis

$$\dot{Q} = \dot{m}(h_{out} - h_{in}) \tag{30}$$

Heat exchanger is sized based on its overall thermal resistance, quantified as 1/UA. UA is related to the total heat transfer by the relation below, where T_{avg} is the log mean temperature.

$$\dot{Q} = UA(\Delta T)_{avg} \tag{31}$$

The log mean temperature with a cold side temperature of 15 C, taken from [5] is can be shown below. It is assumed that the heat rejected was a negligible effect in the cold well temperature across the heat exchanger.

$$\Delta T_{lm} = \frac{\Delta T_R - \Delta T_L}{ln[\frac{\Delta T_R}{\Delta T_L}]} \tag{32}$$

Where $\Delta\ T_R = T_{h_{in}}$ - T_c and $\Delta\ T_L = T_{h_{out}}$ - T_c.

5.5.3 Flow Combination

After each flow is fed through its respective turbine, they need to be combined to be fed into the pump. The equations governing this are

$$\dot{m}_f = \dot{m}_1 + \dot{m}_2 \tag{33}$$

$$\dot{m}_f h_f = \dot{m}_1 h_1 + \dot{m}_2 h_2 \tag{34}$$

Where f designates the final state, and 1 and 2 are the input states. h in this case is the enthalpy.

5.6 Turbomachinery Sizing

Once the system was optimized for power output, the system components had to be sized accordingly. This was done using provided NS-DS charts, which relate Specific Speed to Specific Diameter. Curves representing turbine efficiency were added. The NS-DS charts below were provided.

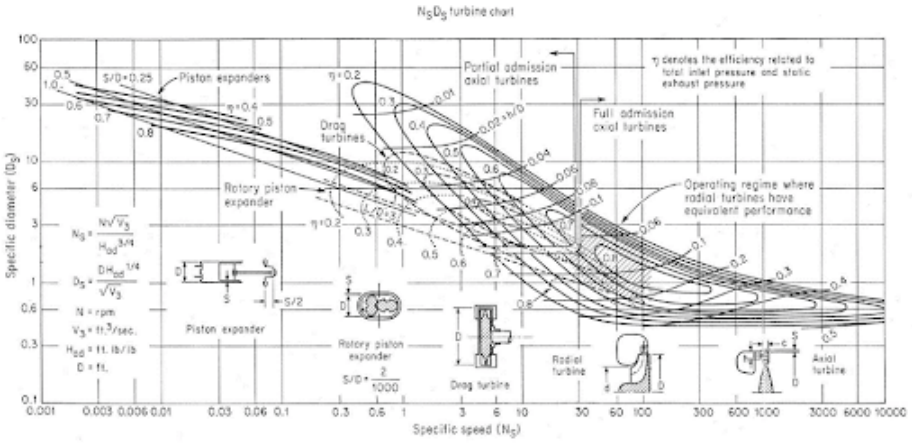

Figure 3: Turbine NS-DS

The equation for Specific Speed on the chart, in all base SI units is

$$N_s = 129\frac{\Omega Q^{\frac{1}{2}}}{\Delta h_s^{\frac{3}{4}}} \tag{35}$$

Where Ω is the rotational speed in rad/s, Q is the volumetric flow rate in m^3/s, and δh_s is the change in enthalpy assuming isentropic conditions.

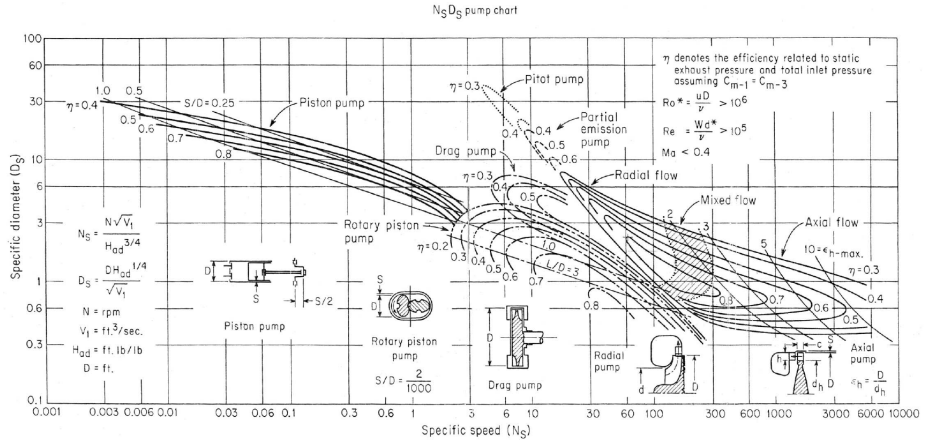

Figure 4: Pump NS-DS

The efficiency of the turbine was calculated using the expression

$$\eta = \frac{P_{out}}{P_{in} + \frac{1}{2}\rho_{in} v_{in}^2} \tag{36}$$

This efficiency was calculated to be 0.5209 and 0.5399 for turbines 1 and 2 respectively. To achieve the desired efficiencies, by inspection of the NS-DS chart, a N_s of approximately 5 is required. Solving for Ω, the turbine angular speed becomes

$$\Omega = \frac{N_s \Delta h_s^{\frac{3}{4}}}{129 Q^{\frac{1}{2}}} \tag{37}$$

The flow parameters of the system and the necessary speed for each turbine is are summarized in the Table 7 below.

Turbine	**Efficiency**	**Q** (m^3/s)	Δh_s **(J/kg)**	**Initial Specific Speed**	**Initial Turbine Speed (rad/s)**
1	0.5209	0.00676	23357	3	534.4
2	0.5399	0.00516	20535	3	555.4

Table 7: Specific Speed Calculations

It was required that the turbines should have a speed that easily integrated into the current power grid. For that reason, the turbine rotational speeds are sized to form clean ratios with 3600 RPM or 376.99 rad/s. The ratios chosen (the gear ratios for the gearboxes), the modified specific speed, and the new rotational speed are summarized below in Table 8.

Turbine	**Gearbox Ratio**	**Operating Speed (rad/s)**	**Specific Speed**
1	3:2	565.5	3.17
2	3:2	565.5	3.05

Table 8: Final Specific Speed Calculations

Given a Specific Speed and a turbine efficiency, a corresponding Specific Diameter can be found on the graph. From a Specific Speed of approximately 3, the required Specific Diameter is approximately 9. The formula for Specific Diameter is given below

$$D_s = \frac{d\Delta h_s^{\frac{1}{4}}}{Q^{\frac{1}{2}}} \tag{38}$$

Rearranging for the desired diameter, d,

$$d = \frac{D_s Q^{\frac{1}{2}}}{\Delta h_s^{\frac{1}{4}}} \tag{39}$$

The parameters and calculated diameters are summarized below in Table 9

Turbine	**Q** (m^3/s)	Δh_s **(J/kg)**	**Diameter (m)**
1	0.00676	23357	0.753
2	0.00516	20535	0.679

Table 9: Diameter Calculations

Likewise for the Pump, the efficiency was calculated by

$$\eta = \frac{P_{in} + \frac{1}{2}\rho_{in} v_{in}^2}{P_{out}} \tag{40}$$

The pump used was a rotary piston pump due to its benefit of being at a lower speed.

Pump	**Efficiency**	**Q** (m^3/s)	Δh_s **(J/kg)**	**Initial Specific Speed**	**Initial Pump Speed (rad/s)**
1	0.60	0.00801	5709.8	6	350.2

Table 10: Specific Speed Variables

As with the turbines, the Specific Speed was modified for an achievable gearbox ratio. The power input for systems in the United States are 3600 RPM.

Pump	**Gearbox Ratio**	**Operating Speed (rad/s)**	**Specific Speed**
1	16:17	354.8	6.08

Table 11: Specific Speed Variables

A Specific Speed of approximately 6.08 correlates to a necessary Specific Diameter of approximately 2. The Specific Diameter was calculated with the values summarized in the Table below.

Pump	**Q** (m^3/s)	Δh_s **(J/kg)**	**Pump Diameter**
1	0.00801	5907.8	0.257

Table 12: Specific Speed Variables

5.7 Solving Methodology

The system was optimized with respect to the following three parameters: near outtake flow rate, far outtake flow rate, and Pump Outlet Pressure. Code was written to compute the entire thermal state, and, ultimately, the net power of the thermodynamic cycle given the three optimization parameters. From there, the solution space was charted to find regions of optimal net positive power. Lastly, a global optimizer was employed to find the optimum inside of the bounds found to be optimal from the charting.

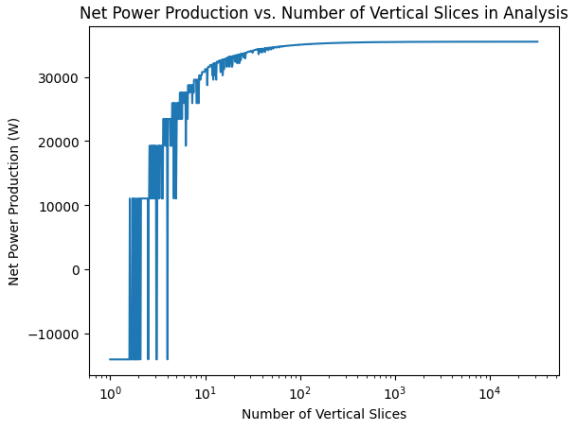

Figure 5: Vertical Slice Study

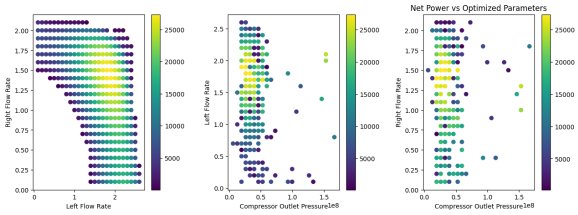

Figure 6: Solution Space Charting

One important meta parameter was the vertical pipe analysis step size. More vertical segments result in a more accurate discrete analysis, but require more computation time, resulting in slower overall optimization. A study into net power output as a function of number of vertical slices was conducted, revealing that 2000 slices was sufficient.

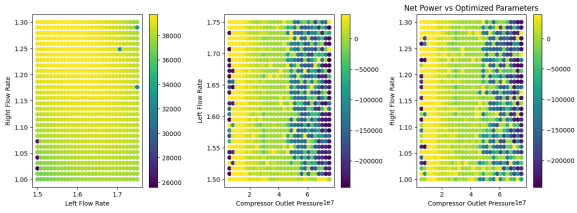

Figure 7: Zoomed in Solution Space Charting

The final Parameters, after optimization resulted in the following conditions, summarized in Table 13

Parameter	Value	Unit
Pump $\dot{m}$	6.27	kg/s
Outtake 1 $\dot{m}$	1.69	kg/s
Outtake 2 $\dot{m}$	1.34	kg/s
Pump Outlet Pressure	10.0	MPa

Table 13: Optimized System Parameters

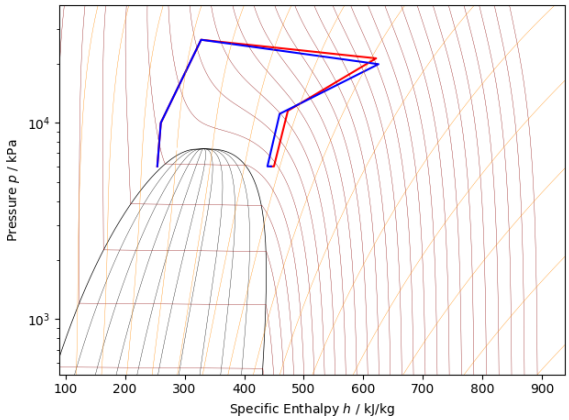

Figure 8: Pressure Enthalpy Chart of Optimal Cycle

These conditions result in the following system parameters, summarized in Table 14

Parameter	Value	Unit
Sequestration Cost	16.3	kW
Pump Draw	31.5	kW
Turbine Power	66.9	kW
Net Power	35.5	kW
Heat Exchanger Sizing	5103	W/K

Table 14: Optimized System Outputs

6 Evaluation

From Table 14 the system produces a net power of 35.5 kW. This is not nearly enough to compete with conventional power plants such as coal or nuclear energy. However, the main benefit of this design is CO_2 sequestration. While the design fails to produce a significant amount of power it sequesters CO_2 helping to lower greenhouse gas emissions. Furthermore, the design does so while creating a positive net power that could power about 30 homes [7]. If one where to sequester the CO_2 without the power cycle it would take 16.3 kW to power the pump. Thus, the system is considered successful with a purposeful implementation.

Another benefit with this design is the already existing infrastructure. In places where CO_2 sequestration is already taking place, the geothermal power cycle could easily be added to existing sequestration wells. This would greatly reduce time and cost compared to building a new power plant.

Research was conducted in an attempt to compare the proposed geothermal-sequestration system to contemporary modules. Unfortunately, the concept is so new that very few to none are currently operational.

That being said, the system developed is optimal given the proposed location, geometry, and goal to maximize power output. As detailed in the Solving Methodology section, all solution spaces and configurations were considered. The design choices logically make sense. A second well uptake pipe was used because the Pressure loss is much less compared to the pressure loss across the porous

formation. Additionally, the heat lost in this pipe is no different than both mass flows going up a single pipe. Combining the two flows after the two turbines is beneficial because as much energy from pressure can be extracted. If the Tee joint was before the turbine, the Pressure balance between the two pipes would limit one pipe's energy potential. With two turbines, the maximum pressure can be extracted from each. As the numbers outlined in the analysis show, one pipe-turbine pathway provides more power, which would be unused otherwise. By fixing the recycled fluid to the properties of the replenishing fluid before the pump is also optimal, as there is no loss of energy due to a difference in fluid properties.

7 References

[1]"Relative Roughness - an overview — ScienceDirect Topics," www.sciencedirect.com. https://www.sciencedirect.com/topics/engineering/relative-roughness#:~:text=%CE%B5%20%3D%20pipe%20absolute%20roughness%2C%20in

[2] C. Guan, Z. Fang, W. Zhang, H. Yao, Y. Man, and M. Yu, "Dynamic Heat Transfer Analysis on the New U-type Medium-Deep Borehole Ground Heat Exchanger," Frontiers in Energy Research, vol. 10, Mar. 2022, doi: https://doi.org/10.3389/fenrg.2022.860548.

[3] "Soil - Hydrological Group," geohub.lacity.org. https://geohub.lacity.org/maps/labos::soil-hydrological-group/explore?location=34.018669%2C-118.410603%2C8.97 (accessed Apr. 23, 2024).

[4] "Thermal conductivity of soil," Cableizer. https://www.cableizer.com/documentation/k_4/ (accessed Apr. 23, 2024).

[5] C. G. S. Temperatures-A.-C. Ltd, "Los Angeles Water Temperature (CA) — United States — Sea Temperatures," World Sea Temperatures. https://www.seatemperature.org/north-america/united-states/los-angeles.htm (accessed Apr. 25, 2024). [6] "4900 Series High Flow T-Type Filter — Norman Filter Company," www.normanfilters.com. https://www.normanfilters.com/4900-series.html (accessed Apr. 26, 2024).

[7] "How much electricity does an American home use?," https://www.eia.gov/. https://www.eia.gov/tools/faqs/faq.php?id=97&t=3 (accessed May 3, 2024).